Design and development of 6-hydrazinonicotinyl-fatty acid-mimetic 99mTc-complex as a potential myocardial imaging agent

Joel González[1,2], María Fernanda García[1], Pablo Cabral[1], Victoria Calzada[1*], Hugo Cerecetto[1*]

[1]*Área de Radiofarmacia, Centro de Investigaciones Nucleares, Facultad de Ciencias, Universidad de la República, Uruguay, [2]Laboratorio de Experimentación Animal, Centro de Investigaciones Nucleares, Facultad de Ciencias, Universidad de la República, Uruguay*

The goal of this work is to identify new fatty acid-mimetic 99mTc-complexes to be used as myocardial imaging agents that allow studying heart abnormalities in high-risk patients. In this sense, we designed a fatty acid-mimetic substructure including an amide moiety that, among other properties, could improve myocardial residence time. A diamide with a chain length of 15 atoms and porting a 6-hydrazinonicotinyl (HYNIC) chelator, and an analog with a short carbon-chain, were prepared with convergent organic synthetic procedures and radiolabeled with 99mTc using tricine as the sole coligand. The *in vivo* proofs of concept were performed using healthy mice. The new 99mTc-complexes were obtained with adequate radiochemical purity. The lipophilicities were in agreement with the length of the chains. While both 99mTc-complexes showed uptake in the myocardial muscle, the designed radiopharmaceutical with the longest chain length had preferential target-uptake and target-retention compared to other complexes described in the bibliography. Further studies, involving imaging assays, synthetic modifications, and assay of new coligands for 99mTc-HYNIC complexes, are currently ongoing.

Keywords: Technetium. Radiopharmaceutical. Myocardial metabolism. Long chain amide.

INTRODUCTION

Coronary artery disease is the main cause of morbidity and mortality in developed countries (Montalescot *et al.*, 2013; Corbett, 1999). Ischemic myocardial damage is produced when cardiac flow is reduced by a partial or total blockage of the coronary arteries that causes a decrease in the supply of oxygen and nutrients, affecting the metabolism of the myocyte (Montalescot *et al.*, 2013). Oxidation of long-chain fatty acids (LCFAs) is employed, as an energy source, in the fasting state by the myocardium decreasing the anaerobic glycolysis, whereas in non-fasting, ischemia, or infarction conditions,

LCFAs oxidation is suppressed and glucose is used as the main energy source (Schwenk *et al.*, 2008; Corbett, 1999). During the aerobic metabolism, LCFAs undergo β-oxidation into the mitochondria, losing two carbons in each oxidation-cycle (Messina, Aras, Dilsizian, 2007). The monitoring of LCFAs metabolism could indicate the health status of the myocardial muscle in normal and pathological situations (Messina, Aras, Dilsizian, 2007). In this sense, several radiolabeled probes have been used for the assessment of altered myocardial perfusion and metabolic function. However, obtaining freely available, fast production radiopharmaceuticals with good metabolic characteristics remains a challenge.
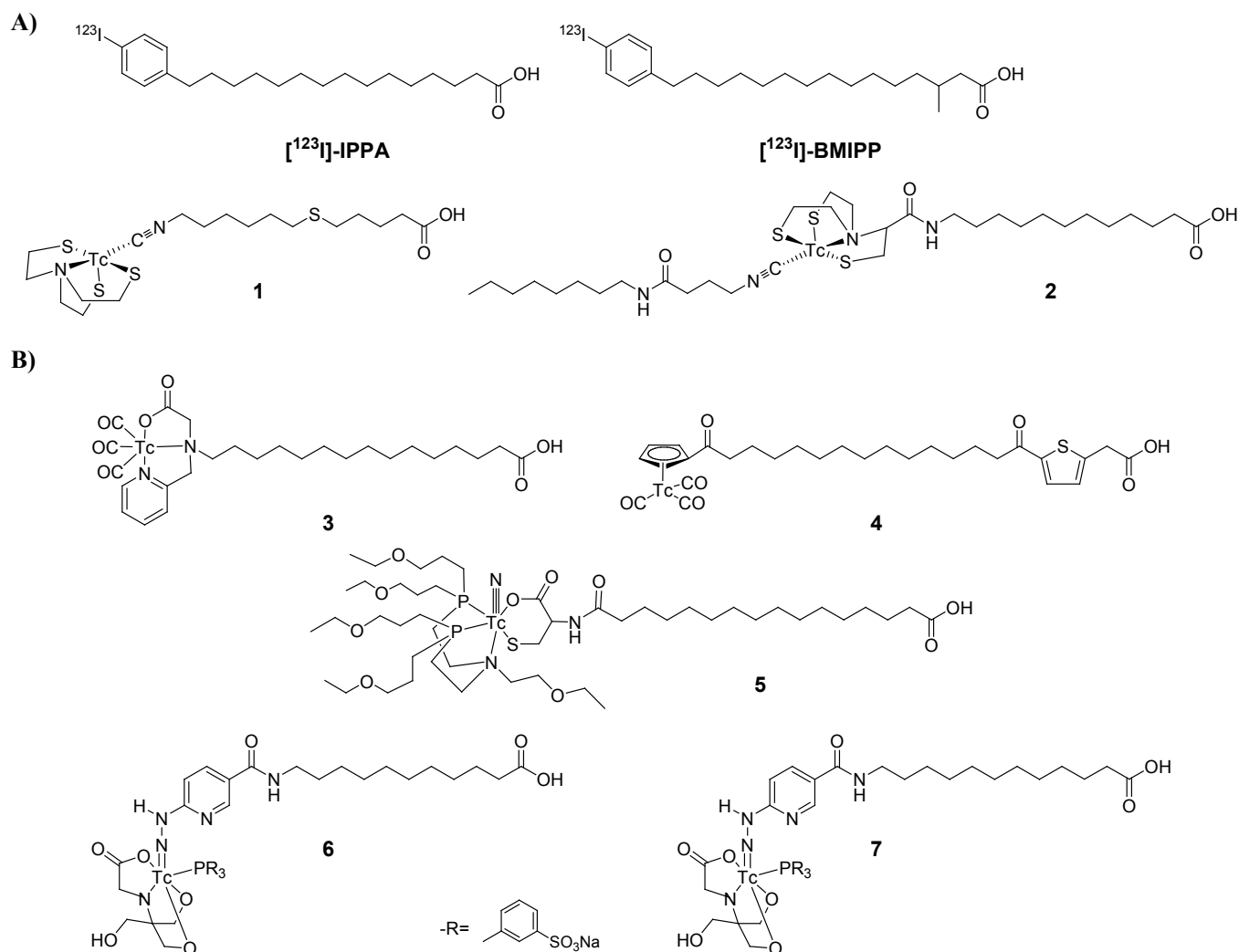
Radiolabeled mimics of LCFAs have been described as markers for detecting alterations in the metabolism of the myocardium (Tamaki *et al.*, 2000), being [123I]-15-(*p*-iodophenyl)pentadecanoic acid one of the first developed agents, known as [123I]-IPPA (Figure 1A) (Machulla *et al.*, 1978). Its main disadvantage is

*Correspondence: V. Calzada. Centro de Investigaciones Nucleares. Facultad de Ciencias, Universidad de la República. Mataojo 2055, 11400 Montevideo, Uruguay. Phone: +598 25250800. E-mail: vcalzada@cin. edu.uy. ORCID: https://orcid.org/0000-0003-2679-8981and H. Cerecetto. Centro de Investigaciones Nucleares. Facultad de Ciencias, Universidad de la República. Mataojo 2055, 11400 Montevideo, Uruguay. Phone: +598 25250800. E-mail: hcerecetto@cin.edu.uy. ORCID: https://orcid.org/0000-0003-1256-3786

its fast myocardium clearance and metabolism (Kaiser *et al.*, 1990). For optimal myocardium imaging, the optimal fatty acid-mimic chain length has been described as 16 or 17 carbon atoms (Otto *et al.*, 1981). On the other hand, LCFAs mimics with improved myocardial residence time have been developed modifying the substitution in the carbon-chain and thus the β-oxidation process, i.e., [^{123}I]-β-methyl-15-(*p*-iodophenyl)pentadecanoic acid, known as [^{123}I]-BMIPP, **1** and **2** (Figure 1A) (Mirtschink *et al.*, 2009a; Mirtschink *et al.*, 2009b; Knapp, Ambrose, Goodman, 1986). Particularly, ^{99m}Tc-complex **2** showed the highest preferential heart subsarcolemmal and intermyofibrillar mitochondria distribution due to the presence of two NH-amide moieties able to interact with membrane surfaces through hydrogen bonds, according to the authors that studied its biology (Mirtschink *et al.*, 2009b). In addition, other ^{99m}Tc-complexes that mimic fatty acids to be used as myocardial imaging agents have been developed, i.e., **3-7** (Figure 1B) (Mathur *et al.*, 2015; Zeng, Zhang, 2014; Mathur *et al.*, 2008; Lee *et al.*, 2007). In these cases, different cores, chelates and coligands have been explored. Among these, the use of 6-hydrazinopyridine-3-carboxyl, also known as

6-hydrazinonicotinyl (HYNIC), has been insufficiently studied (Mathur *et al.*, 2015). In addition to avoiding rapid cardiac clearance, another attribute of interest for a single-photon emission computed tomography radiopharmaceutical is a favorable heart:liver ratio, as the radioprobe is eliminated via the hepatic pathway, which may affect the resolution of myocardium images.

Considering this background, the purpose of our study was to identify new fatty acid-mimetic ^{99m}Tc-complexes to be used as myocardial imaging agents. Herein, we describe the design of a new LCFAs mimic, **8**, able to coordinate ^{99m}Tc, via HYNIC chelator, obtaining a potential myocardial imaging agent. In the design (Figure 2), we considered a long carbon-chain that includes two amide moieties in order to promote the interactions with membrane surfaces and avoid complete β-oxidation, improving the residence time in the cardiac muscle. This ligand was coordinated to the metallic radionuclide ^{99m}Tc using tricine as a coligand to generate a radiopharmaceutical, **Tc-8** (Figure 2), with adequate hydrophilicity to minimize liver biodistribution. *In vivo* proofs of concept were done with the generated radioprobe **Tc-8** and using an analog, **Tc-9**, with a short carbon-chain (Figure 3).

FIGURE 1 - A) LCFAs mimics with improved myocardial residence. **B)** Potential myocardial imaging radiopharmaceuticals with coordinated-^{99m}Tc sub-structure. Note: In all cases, Tc refers to the ^{99m}Tc radionuclide.

MATERIAL AND METHODS

Material

6-(*t*-Butyloxycarbonylamino)hexanoic acid and *N*-succinimidyl 6-(*t*-butyloxycarbonylhydrazino) nicotinic acid were synthesized as described in the literature (Calzada *et al.*, 2017; García *et al.*, 2014;

Gavande *et al.*, 2013). All chemicals and solvents were purchased from Sigma-Aldrich, Mallinckrodt, Merck, Biopack, and Química Gamma. All solvents for organic synthesis were dried and distilled prior to use. Water was purified and deionized (18 MΩ/cm²) on a Milli-Q water filtration system (Millipore Corp., Milford, MA). ^{99}Mo-^{99m}Tc generators were purchased from TecnoNuclear (Argentina).
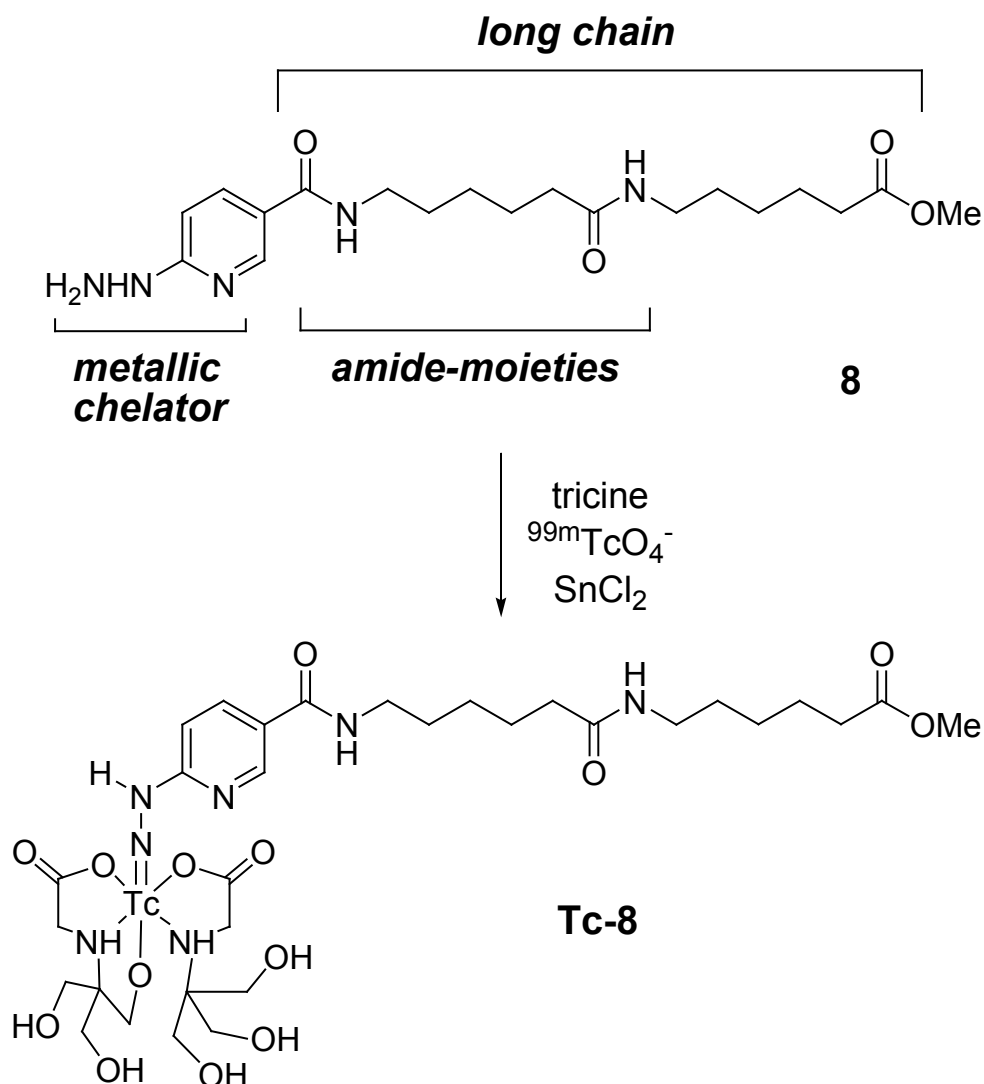
FIGURE 2 - Design of the new HYNIC-fatty acid-mimetic ^{99m}Tc-complex developed in this study.

Equipments

Analytical TLC was performed on SiO_2 plates (Alugram® Sil G/UV254) or Al_2O_3 plates (Poligram® Alox N/UV254) and visualized with UV light (254 nm) or I_2 vapor. Preparative chromatographies were performed on SiO_2 (Kieselgel®, 0.063-0.2 mm, JT Baker) or Al_2O_3 (Neutral Alumina AG 7®, 100-200 mesh, Bio Rad).

Structural elucidations were based on ^{1}H, ^{13}C, COSY, HMBC, and HSQC spectroscopies, and MS spectrometry. NMR spectra were acquired on a Bruker DPX 400 (400 MHz) spectrometer. The chemical shifts values were expressed in ppm relative to tetramethylsilane as the

internal standard. Mass spectra were determined on a Shimadzu GCMS-QP 2010 ULTRA spectrometer using electronic impact ionization (EI, 70 eV).

Reverse-phase high-performance liquid chromatography (RP-HPLC) was performed on an Agilent 1200 Series Infinity Star equipped with a GABI Star detector, a UV detector and a ThermoScientific Hypersil ODS reverse-phase C_{18} column (300 mm × 4.6 × 10 microns). Radio-TLC detection was accomplished using instant thin-layer chromatography (ITLC) on silica gel strips (Pall Corporation, Port Washington, NY).

Radioactivity was counted in a CRC-7 Capintec dose calibrator and in a solid scintillation counter detector with

a 3"×3" NaI(Tl) crystal associated with a single channel analyzer (ORTEC, Oak Ridge, TN).

Animals

Balb/c female mice, of 19-25 g body weight, were produced and provided by *Unidad de Reactivos para Biomodelos de Experimentación* (URBE), *Facultad de Medicina*, *Universidad de la República* (Montevideo, Uruguay). The authors state that they followed the principles outlined in the Declaration of Helsinki for all animal experimental investigations. Animals were housed in wire mesh cages at 20 ± 2 ºC, with 12 h artificial light-dark cycles. The animals were fed *ad libitum* to a standard pellet diet and water and were used after a minimum of 3 days of acclimation to the housing conditions. The animals were kept fasting for 6-7 h prior to the experiment with water *ad libitum*.

All protocols for animal experimentation were conducted in compliance with the procedures authorized by the Ethical Committee for Animal Experimentation, *Universidad de la República* (Montevideo, Uruguay), by whom this project was previously approved, and the research adhered to the Principles of Laboratory Animal Care (Morton, Griffiths, 1985).

Data analysis

All data are presented as means±S.D. Statistical analyses were performed using Student's unpaired 2-tailed *t* test for the comparison of two groups.

Methods

Synthesis of methyl 6-[6-(6-t-butyloxycarbonylhydrazinonicotinylamino) hexanoylamino] hexanoate (8-Boc)

Methyl 6-aminohexanoate. A mixture of 6-aminohexanoic acid (500 mg, 4.3 mmol), dry methanol (10 mL), and concentrated sulfuric acid (catalytic amount) was heated at reflux, under N_2 atmosphere, in a vessel (25 mL) connected to a closed dropping funnel (10 mL), with a pressure equalizing tube, charged with molecular sieves

3 Å and dry methanol (8 mL). When the methanol volume in the dropping funnel reached 10 mL, the funnel was opened to discharge the solvent to the flask and closed to repeat the refluxing cycle. The reaction mixture was heated for 24 h. The solvent was evaporated *in vacuo* and the residue was treated with a saturated aqueous solution of NaHCO$_3$ (25 mL) and CH$_2$Cl$_2$ (50 mL × 3). The organic phase was filtered through celite, dried with Na$_2$SO$_4$, and evaporated *in vacuo* to yield the desired product (brown oil, 68 % yield).

Methyl 6-[6-(t-butyloxycarbonylamino) hexanoylamino]hexanoate. A mixture of 6-(*t*-butyloxycarbonylamino)hexanoic acid (1 equiv), thionyl chloride (10 equiv), dimethylformamide (DMF) (0.1 equiv), and dry CH$_2$Cl$_2$ was heated at reflux, under N_2 atmosphere, for 15 min. The solvent was evaporated *in vacuo*, and the residue, at 0 ºC, was treated with Et$_3$N (15 equiv) and methyl 6-aminohexanoate (1 equiv) dissolved in dry CH$_2$Cl$_2$. The reaction was stirred at room temperature for 2 h. The mixture was treated with a saturated aqueous solution of NaCl and ethyl acetate (× 10). The organic phase was dried with Na$_2$SO$_4$ and evaporated *in vacuo* to yield a crude that was purified by column chromatography (SiO$_2$, ethyl acetate:methanol (0 to 10 %)) obtaining the desired product (yellow oil, 18 % yield).

Methyl 6-[6-(6-t-butyloxycarbonylhydrazino nicotinylamino)hexanoylamino]hexanoate (8-Boc). A mixture of methyl 6-[6-(*t*-butyloxycarbonylamino) hexanoylamino]hexanoate (30.4 mg, 0.085 mmol), trifluoroacetic acid (TFA) (127.2 µL) and CH$_2$Cl$_2$ (2 mL) was stirred at room temperature, under N_2 atmosphere, for 2 h. The reaction was treated with water (20 mL) and ethyl acetate (100 mL × 10). The organic phase was dried with Na$_2$SO$_4$ and evaporated *in vacuo* to yield methyl 6-(6-aminohexanoylamino) hexanoate (yellow oil, 90 % yield). A mixture of methyl 6-(6-aminohexanoylamino)hexanoate (1 equiv), *N*-succinimidyl 6-(*t*-butyloxycarbonylhydrazino)nicotinic acid (1 equiv), Et$_3$N (22 equiv), and dried tetrahydrofuran (THF) was stirred at room temperature, under N_2 atmosphere, for 16 h. The solvent was evaporated *in vacuo* and the residue was treated with water and ethyl acetate (× 3). The organic phase was dried with Na$_2$SO$_4$

and evaporated *in vacuo* to yield a crude that was purified by column chromatography (SiO$_2$, ethyl acetate:petroleum ether (7:3)) obtaining the desired product **8-Boc** (brown oil, 50 % yield). ^{1}H NMR (CDCl$_3$): δ 11.87 (bs, 3H), 9.18 (bs, 1H), 8.87 (d, J = 1.9 Hz, 1H), 8.18 (dd, J = 8.9, 1.9 Hz, 1H), 6.80 (d, J = 8.6 Hz, 1H), 3.67 (s, 3H), 3.07 – 2.97 (m, 4H), 2.36 – 2.20 (m, 4H), 1.76 – 1.54 (m, 12H), 1.47 (s, 9H). EI-MS, *m/z* (%): 460 (M$^{+\cdot}$ − CH$_3$O$^\cdot$ − H$_2$, 7), 294 (15), 277 (10), 86 (C$_4$H$_5$NO$^+$, 100).

Methyl 6-(6-t-butyloxycarbonylhydrazinonicotinylamino)hexanoate (9-Boc)

A mixture of methyl 6-aminohexanoate (1 equiv), *N*-succinimidyl 6-(*t*-butyloxycarbonylhydrazino)nicotinic acid (1 equiv), Et$_3$N (5 equiv), and dried THF was stirred at room temperature, under N$_2$ atmosphere, for 24 h. The solvent was evaporated *in vacuo* and the residue was treated with water and ethyl acetate (× 3). The organic phase was dried with Na$_2$SO$_4$ and evaporated *in vacuo* to yield a crude that was purified by column chromatography (SiO$_2$, ethyl acetate:petroleum ether (7:3)) obtaining the desired product **9-Boc** (brown oil, 35 % yield). ^{1}H NMR (CD$_3$COCD$_3$): δ 8.63 (d, J = 2.2 Hz, 1H), 8.13 (bs, 1H), 8.03 (dd, J = 8.8, 2.0 Hz, 1H), 7.77 (bs, 1H), 7.60 (bs, 1H), 6.71 (d, J = 8.7 Hz, 1H), 3.61 (s, 3H), 3.38 (dd, J = 12.8, 6.9 Hz, 2H), 2.32 (t, J = 7.4 Hz, 2H), 1.45 (s, 9H), 1.43 – 1.35 (m, 6H). EI-MS, *m/z* (%): 347 (M$^{+\cdot}$ − CH$_3$O$^\cdot$ − H$_2$, 5), 86 (C$_4$H$_5$NO$^+$, 100), 57 (40).

^{99m}Tc-Radiolabeling. Synthesis of Tc-8

A mixture of **8-Boc** and TFA was stirred at room temperature, under N$_2$ atmosphere, for 24 h. The reaction solvent was evaporated *in vacuo* to yield **8-TFA** that was used in the next reaction without further purification. An aqueous solution of tricine (1 mg/mL, 29 µL, 0.164 mmol) was added to a solution of **8-TFA** (40 µg, 0.082 µmol) in NaCl 0.9 %. After that, a fresh solution of SnCl$_2$ · 2 H$_2$O (0.1 M in HCl, 19 µL, 0.082 mmol) and a saline solution of Na^{99m}TcO$_4$ (74-296 MBq, 100 mL), from the generator ^{99}Mo-^{99m}Tc, were added. The pH of the solution was adjusted to 4.5-5.0. The mixture was incubated for 60 min at 75 °C in a dry bath. Labeling efficiency was determined using RP-HPLC with a 20 min gradient and a flow rate of 1mL/min. Mobile phases (A) water/0.1%

TFA and (B) acetonitrile/0.1% TFA (0-10 min 0-45% B,) 10-20 min 45-65% B) were used. SEP-PAK$^®$ c18 cartridge (Waters) was used to quantify ^{99m}Tc-colloidal.

Synthesis of Tc-9

Similar experimental conditions used to prepare **Tc-8** were employed for the synthesis of **Tc-9**.

Physicochemical properties
Distribution coefficient

Log$_{10}$ $D_{7.4}$ values were determined in triplicate as follows: the radiolabeled products were purified by RP-HPLC, as described before, and an appropriate amount of the corresponding probe, **Tc-8** or **Tc-9**, was incubated and vigorously mixed in a mixture of phosphate-buffered saline (PBS) (0.01 M, pH 7.4, 500 µL) and *n*-octanol (500 µL) for 1 min. After that, the mixture was centrifuged at 3,000 rpm for 5 minutes. Three fractions of 100 µL were collected from both phases of each tube, and the radioactivity was counted in a NaI well counter. The distribution coefficient was obtained as log$_{10}$ (*n*-octanol counts/aqueous phase counts).

In vivo proof of concept. In vivo biodistribution of Tc-8 and Tc-9

After the RP-HPLC purification of both probes, **Tc-8** and **Tc-9**, they were diluted with 500 µL of 0.1 M phosphate buffer (PB) pH 7.4, and the acetonitrile was reduced by applying a N$_2$ flow. Finally, 0.1 M PB pH 7.4 was added as needed to achieve a neutral pH. Each probe was injected intravenously (10-22 MBq in 50µL of saline), via tail, on Balb/c mice. The animals (4 mice per time point) were sacrificed by cervical dislocation at 2, 5, 10, 30, 60, and 120 min post-injection (PI). The organs and tissues of interest were dissected and weighed, and the radioactivity of the samples was measured in a gamma counter. Radioactivity in the urine and feces was also determined. The radioactivity was expressed as percent injected dose per gram of organ weight (% ID/g) or percent of injected dose (% ID). The total amount of blood was considered as 6.5 % of the total body weight.

RESULTS AND DISCUSSION

Synthesis of long chain fatty acid-mimic ligands

Two LCFA-mimic ligands, **8** and **9**, with chain lengths of 15 and 8 atoms, respectively, were synthesized following the steps shown in Figure 3. In position 15 and 8, respectively, the 6-hydrazinopyridine-3-yl (6-hydrazinonicotinyl) system was located to allow radiolabeling with ^{99m}Tc. To prepare the trifluoroacetyl-derivative of **8**, **8-TFA** (Figure 3), we used a convergent procedure from the starting material 6-aminohexanoic acid, which was protected, on the one hand, as methyl ester and, on the other hand, as *N*-(*t*-butyloxycarbonyl) amide (*N*-Boc-amide). After that, both protected reactants were coupled by carboxylic acid activation with thionyl chloride. Finally, after Boc-deprotection, the amine was reacted with succinimidyl 6-Boc-hydrazinonicotinic acid (García *et al.*, 2014), yielding **8-Boc**. The treatment of this product with TFA, just before radiolabeling, yielded **8-TFA**. Similarly, a short carbon-chain analog was prepared, yielding **9-TFA** (Figure 3). All the intermediates and final products were characterized by NMR techniques and EI-MS spectrometry.

^{99m}Tc-radiolabelled of long chain fatty acid-mimic ligands

LCFA-mimic ligands, **8-TFA** and **9-TFA**, were subsequently radiolabeled with ^{99m}Tc, as mentioned in the Materials & Methods section. In the radiolabeling conditions, the trifluoroacetylhydrazine group was deprotected and subsequently reacted with ^{99m}Tc and the coligand to yield **Tc-8** and **Tc-9** (García *et al.*, 2014). Tricine was the coligand used, selected in order to stabilize the complexes (Meszaros *et al.*, 2010). The radiolabeled processes were checked by chromatography (Figure 4A), obtaining the desired products in radiochemical yields of 82-90 %, purifying them by analytical RP-HPLC.

Because lipophilicity is a very crucial radiopharmaceutical physicochemical property, related to passive diffusion, we determined **Tc-8** and **Tc-9** distribution coefficients between *n*-octanol and PBS (pH 7.4), and the $\log_{10} D_{7.4}$ was used as the measure of its lipophilicities (Figure 4B). As we expected, for the coligand used (tricine), both radiopharmaceuticals were hydrophilic, and a clear correlation between the chain length and $\log_{10} D_{7.4}$ was observed, being **Tc-8** the most hydrophobic radiopharmaceutical with the largest atom-chain.
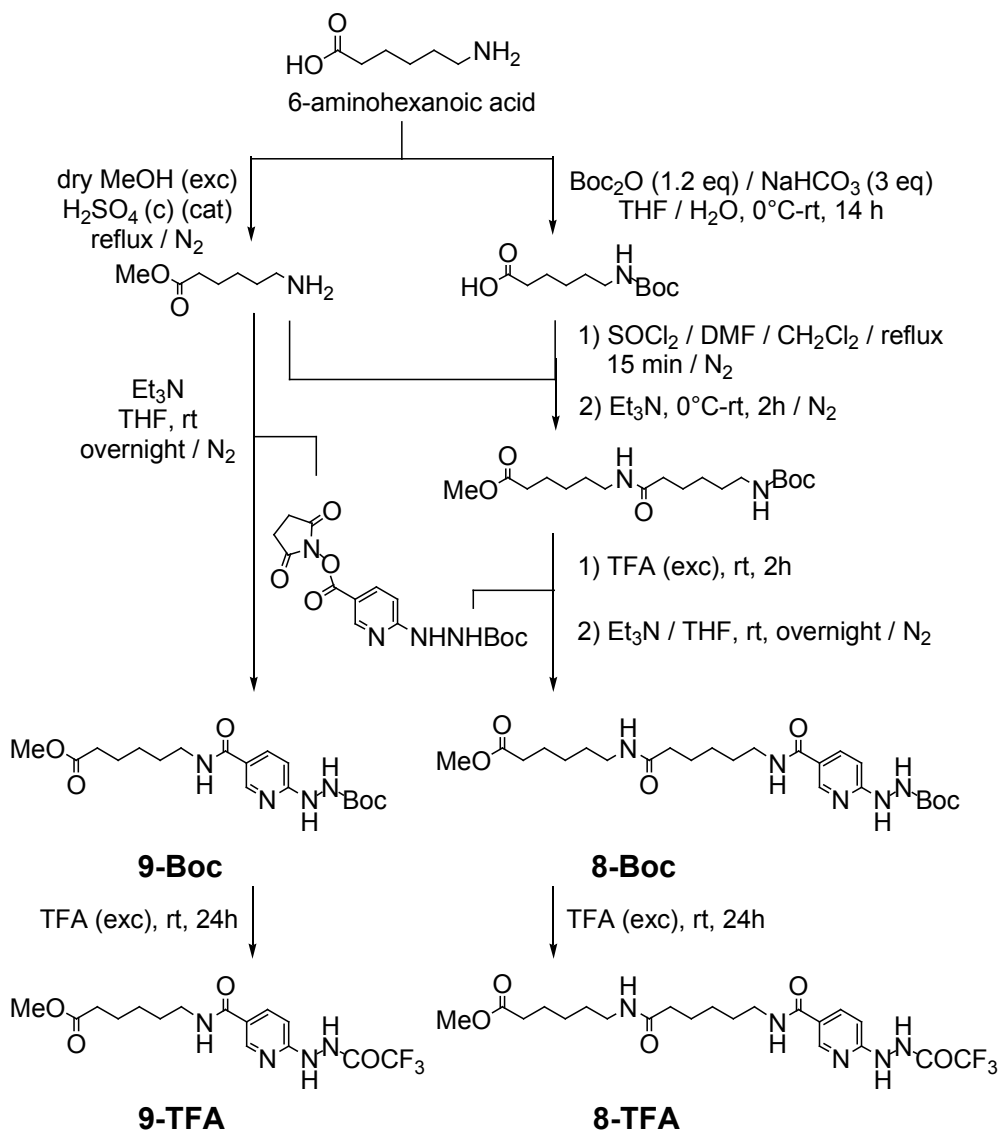
Figure 3 - Convergent synthesis of **8-TFA** and its short carbon-chain analog, **9-TFA**.

Compd.	Tc-8	Tc-9
$\log_{10} P_{o/w}$	-1.05 ± 0.21	-1.23 ± 0.03
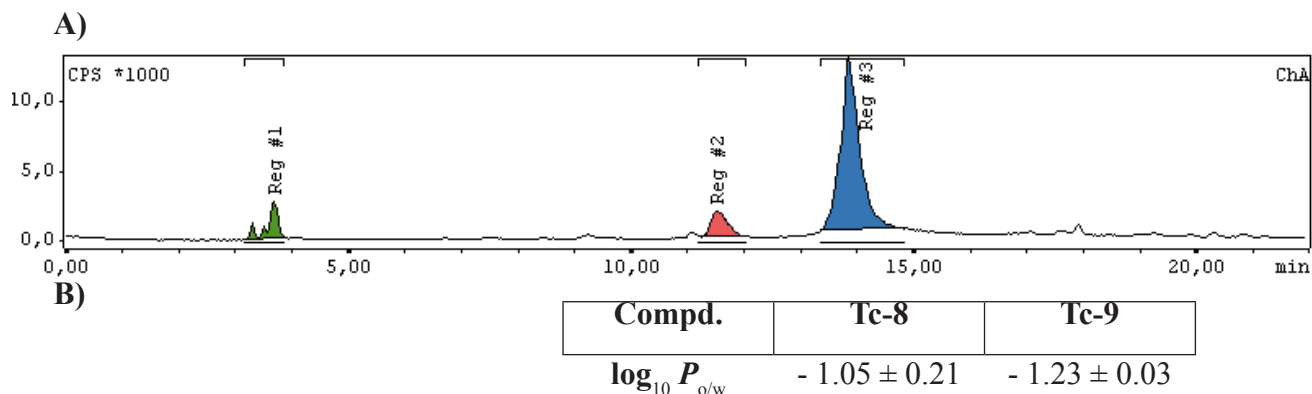
FIGURE 4 - A) Example of RP-HPLC analysis of radiolabeling mixture. Green area: ^{99m}Tc-tricine complexes; Red area: secondary product; Blue area: **Tc-9**. **B)** Values of determined $\log_{10} D_{7.4}$ for developed radiopharmaceuticals.

In vivo proof of concept

The RP-HPLC purified complexes **Tc-8** and **Tc-9** were injected in normal female BALB/c mice, and biodistribution studies were performed between 2 to 120 minutes (Table I). Radiopharmaceuticals displayed the maximum myocardium uptake at 2 minutes PI, being 5.15 ± 0.54 %ID/g for **Tc-8** and 3.33 ± 0.80 %ID/g for **Tc-9**, both significantly different between each other ($p < 0.14$). The elimination of compounds was fast appearing (2 min PI) in the bladder and urine. Myocardial and skeletal muscles uptakes of both compounds are shown in Figure 5. **Tc-8**, for 2, 5, and 10 min, showed significantly better uptake in the myocardium than in skeletal muscle, and significantly decreased heart-radioactivity during that time (Figure 5A). On the other hand, **Tc-9** showed constant myocardium uptake during the time up to 120 min PI, and, like **Tc-8**, significantly better heart-uptake than in skeletal muscle for 5, 30, and 60 min (Figure 5B).

Regarding target:non-target ratios for thoracic relevant organs, we analyzed the biodistributions of myocardium with respect to liver and lungs, and additionally with respect to blood and skeletal muscle, in order to compare the values between both probes, i.e., **Tc-8** and **Tc-9** (Table II). The myocardium:thoracic organs ratios were, for both radiopharmaceuticals, lower than the unit at all the analyzed times. In general, the myocardium:liver and myocardium:lungs ratios for **Tc-8** were constant during the assayed point times. On the other hand, while the myocardium:liver ratios were constant for **Tc-9** over time, the myocardium:lungs ratios increased significantly with time starting at 5 min PI. For **Tc-8**, the myocardium:liver ratios were significantly higher at 2 and 5 min PI than those for **Tc-9**. Regarding the myocardium:skeletal muscles ratios, we could conclude that both compounds had no difference at 2 and 5 min PI, while **Tc-9** significantly displayed the maximum ratio at 30 min PI. Except for the first measurement time (2 min), the myocardium:blood ratios were not significantly different between **Tc-8** and **Tc-9**. Observing the variation of the myocardium:skeletal muscle and myocardium:blood ratios over time, it was possible to observe the significant clearance from the heart to the peripheral blood with time.

The preferential myocardium-biodistribution for **Tc-8** with respect to **Tc-9** could be attributed to the highest lipophilicity of the first complex (Figure 4), which resulted in the highest uptake in the heart muscle (Table I).

CONCLUSIONS

Tc-8, a new fatty acid-mimetic ^{99m}Tc-complex, was designed and synthesized in good yield > 82 %, using HYNIC as a technetium chelator and tricine as a coligand (Calzada *et al.*, 2017; Mathur *et al.*, 2015; García *et al.*, 2014; Zeng, Zhang, 2014; Mathur *et al.*, 2008; Lee *et al.*, 2007). The proof of concept using healthy mice demonstrated that the potential radiopharmaceutical **Tc-8** shows adequate myocardial uptake and target organ-retention. While the uptake and retention of the probe is important for myocardial imaging, other properties, such as clearance of the radiotracer from the background organs (i.e., liver, lungs or blood), play an important role for obtaining good contrast images. In this sense, when we compare our potential radioprobe, **Tc-8**, or its short carbon-chain analog, **Tc-9**, with the other described (Mathur *et al.*, 2015) fatty acid-mimetic ^{99m}Tc-HYNIC-tricine-complexes, **6** and **7** (Figure 1B), we could highlight the following (Table III): i) Our radioprobes displayed better myocardium uptake at 2 min PI than **6** and **7**; ii) after 30 min of injection, our radioprobes remained in the target organ better than **6** and **7**; iii) after 30 minutes of probe-biodistributions, the clearance to the background organs was worse for **6** and **7** than for our radioprobes, observing higher, or similar, ratios for **Tc-8** and **Tc-9**, being thoracic organ liver the worst for compounds **6** and **7**. These behaviors could be the result of: i) the use of the amide connector in **Tc-8** that slowed down its β-oxidation, increasing myocardium-retention; ii) the use of tricine as the sole coligand in **Tc-8** and **Tc-9**, which conferred adequate probe-lipophilicities, unlike probes **6** and **7** that also possess a triphenylphosphine coligand in their structure.

**TABLE I -** Biodistribution studies of **Tc-8** and **Tc-9** complexes in healthy Balb/c mice

	Tc-8				Tc-9				
	%ID/g[(1),(2)]				%ID/g[(1),(`2)]				
	2 min	5 min	10 min	30 min	2 min	5 min	30 min	60 min	120 min
Heart	5.15±0.54 [a]	3.77±0.76 [b]	2.94±0.62	1.17±0.31 [c]	3.33±0.80 [a]	1.64±0.14 [b]	2.91±1.18 [c]	3.36±0.54	1.79±1.14
Liver	17.7±2.9	16.8±3.6 [d]	13.05±0.02	5.95±2.99 [e]	27.4±6.6	30.1±6.1 [d]	15.4±1.1 [e]	19.1±6.4	10.5±4.0
Lungs	13.9±2.5	6.79±0.65	6.51±1.32	4.01±1.33 [f]	9.82±2.37	6.57±3.17	5.99±0.43 [f]	5.23±0.62	2.72±2.28
Muscle	1.80±0.53	1.52±0.63 [g]	1.42±0.41	1.13±0.27	1.22±0.29	0.71±0.07 [g]	0.90±0.54	0.89±0.40	1.89±1.03
Spleen	15.0±3.6	16.7±2.0	17.9±0.1	2.85±1.81	14.4±3.5	13.3±3.5	9.08±2.20	7.70±1.58	3.49±0.80
Kidneys	17.0±0.8	14.4±1.6	12.3±1.7	8.86±3.99	26.6±15.1	15.2±0.7	31.2±7.6	16.1±0.6	5.80±2.53
Stomach	3.70±0.52	7.27±0.79	6.74±2.20	13.3±2.1	1.16±0.28	15.2±3.8	9.62±0.18	8.36±3.13	2.93±0.03
Gut	2.03±0.22	1.83±0.13	2.24±0.03	3.07±0.62	2.16±0.52	4.05±0.48	6.74±2.12	9.09±1.74	8.38±4.32
Bones	3.12±0.47	2.49±0.84	1.88±0.53	1.28±0.30	2.10±0.51	1.24±0.81	2.26±0.73	3.04±0.71	1.81±0.66
Blood	7.32±0.22[h]	13.9±3.8 [i]	12.3±1.7	3.88±0.86	1.39±0.34 [h]	3.35±3.66 [i]	6.30±2.86	8.61±2.89	8.37±3.95
	%ID[(1),(2)]				%ID[(1),(2)]				
Bladder+urine	19.3±2.8 [j]	17.0±8.5	24.1±4.7	29.8±10.4	7.13±1.04 [j]	18.3±3.5	39.0±1.9	28.8±7.6	52.8±11.0

[(1)] Values are given as means ± SD of groups of 4 mice. [(2)] Same letters in each row represent significantly different data comparing probes **Tc-8** and **Tc-9** (for the relevant organs, i.e., heart, liver, lungs, muscle, blood and bladder+urine): (a) $p < 0.14$; (b) $p < 0.20$; (c) $p < 0.12$; (d) $p < 0.15$; (e) $p < 0.03$; (f) $p < 0.12$; (g) $p < 0.19$; (h) $p < 0.01$; (i) $p < 0.11$; (j) $p < 0.08$.

TABLE II - Relevant organs uptake-ratios for **Tc-8** and **Tc-9**

	Tc-8				Tc-9				
ratio[(1)]	2 min	5 min	10 min	30 min	2 min	5 min	30 min	60 min	120 min
Heart:Liver	0.29±0.01 [a]	0.24±0.10 [b]	0.23±0.05	0.24±0.14	0.12±0.01 [ac]	0.06±0.01 [bc]	0.17±0.10	0.18±0.04	0.18±0.11
Heart:Lungs	0.37±0.03 [d]	0.44±0.11	0.45±0.01 [d]	0.31±0.11	0.34±0.01 [e]	0.28±0.11 [f]	0.49±0.22	0.64±0.03 [ef]	0.81±0.57
Heart:Muscle	2.95±0.57 [g]	2.61±0.49 [h]	2.23±1.07	1.03±0.12 [ghi]	2.72±0.02 [j]	2.34±0.42 [k]	5.17±5.49 [i]	4.62±3.03 [l]	0.54±0.27 [jkl]
Heart:Blood	0.71±0.11 [mnop]	0.24±0.08 [n]	0.24±0.01 [o]	0.31±0.08 [p]	2.40±0.01 [mqrs]	1.17±1.24	0.57±0.42 [q]	0.45±0.26 [r]	0.23±0.15 [s]

[(1)] Same letters in each row represent significantly different data (comparing times and radiopharmaceuticals **Tc-8** and **Tc-9**): (a) $p < 0.01$; (b) $p < 0.10$; (c) $p < 0.01$; (d) $p < 0.11$; (e) $p < 0.01$; (f) $p < 0.13$; (g) $p < 0.13$; (h) $p < 0.03$; (i) $p < 0.03$; (j) $p < 0.01$; (k) $p < 0.06$; (l) $p < 0.15$; (m) $p < 0.03$; (n) $p < 0.05$; (o) $p < 0.10$; (p) $p < 0.06$; .(q) $p < 0.02$; (r) $p < 0.01$; (s) $p < 0.01$.

A)

B)
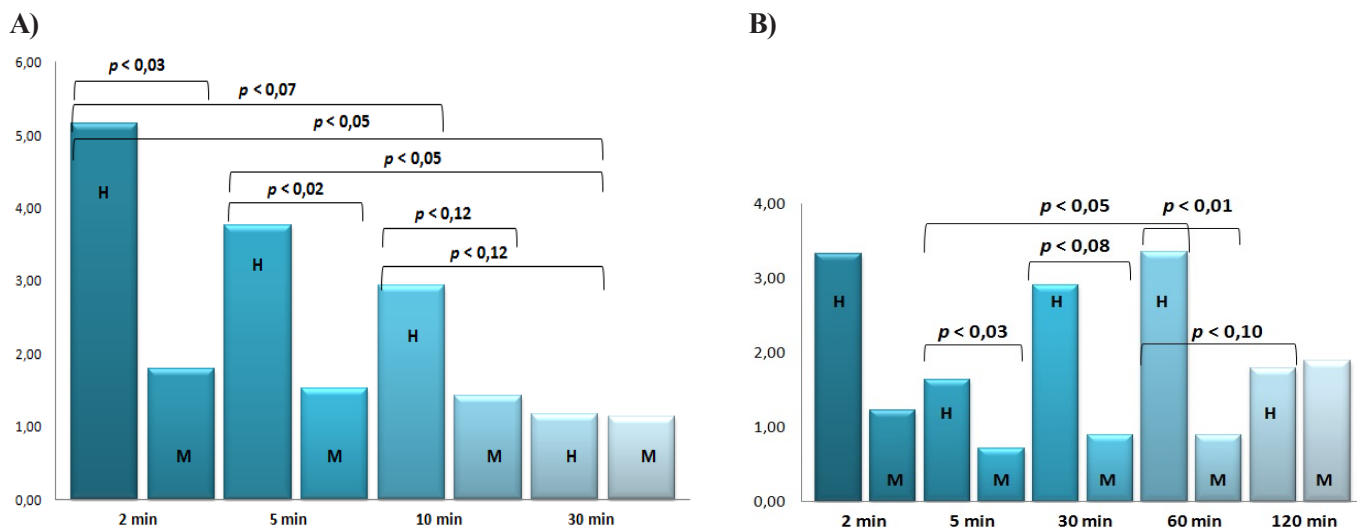
FIGURE 5 - Myocardial (H) and skeletal (M) muscles uptakes of **Tc-8** (**A**) and **Tc-9** (**B**).

TABLE III - Comparison between the radiopharmaceuticals described in this study, **Tc-8** and **Tc-9**, and previously described ones, i.e., **6** and **7**

	ratio at 2 min PI			%ID/g of heart at 2 min PI	$\log_{10} P_{o/w}$
	Heart:Liver	**Heart:Lungs**	**Heart:Blood**		
6[1]	0.08	0.46	0.30	4.87(0.26)	-0.31
7[1]	0.05	0.63	0.54	2.79(0.40)	-0.12
Tc-8	0.29	0.37	0.71	5.15(0.54)	-1.05
Tc-9	0.12	0.34	2.40	3.33(0.80)	-1.23

	ratio at 30 min PI			%ID/g of heart at 30 min PI	
	Heart:Liver	Heart:Lungs	Heart:Blood		
6[1]	0.03	0.41	0.27	0.83(0.31)	
7[1]	0.04	0.28	0.33	0.32(0.06)	
Tc-8	0.24	0.31	0.31	1.17(0.31)	
Tc-9	0.17	0.49	0.57	2.91(1.18)	

[1] Data from reference (Mathur *et al.*, 2015).

The results encourage further studies. Quantitative comparison for more time points for previously reported probes should be complemented with further studies, and imaging studies in a selected animal model should be also performed.

In summary, the present study opens the possibility to study the relevance of screening new HYNIC-fatty acid-mimetic 99mTc-complexes for heart imaging.

ABBREVIATIONS

Boc, *t*-butyloxycarbonyl; DMF, dimethylformamide; HYNIC, 6-hydrazinonicotinyl; [123I]-BMIPP, [123I]-β-methyl-15-(*p*-iodophenyl)pentadecanoic acid; %ID/g, percent injected dose per gram of organ weight; [123I]-IPPA, [123I]-15-(*p*-iodophenyl)pentadecanoic acid; LCFAs, long chain fatty acids; PBS, phosphate-buffered saline; PI, post-injection; RP, reverse phase; TFA, trifluoroacetic acid; THF, tetrahydrofuran.

CONTRIBUTORS LIST

JG, MFG, and VC conducted the research; PC, VC, and HC designed the research and experiments; PC, VC, and HC analyzed the data; PC, VC, and HC wrote the paper. All authors read and approved the final version of the manuscript.

CONFLICTS OF INTEREST

The authors declare no conflict of interest.

ACKNOWLEDGEMENTS

REFERENCES

Calzada V, Moreno M, Newton J, González J, Fernández M, Gambini JP, et al. Development of new PTK7-targeting aptamer-fluorescent and -radiolabelled probes for evaluation as molecular imaging agents: Lymphoma and melanoma *in vivo* proof of concept. Bioorg Med Chem. 2017;25(3):1163-71.

Corbett JR. Fatty acids for myocardial imaging. Semin Nucl Med. 1999;29(3):237-58.

García MF, Calzada V, Camacho X, Goicochea E, Gambini JP, Quinn TP, et al. Microwave-assisted synthesis of HYNIC protected analogue for 99mTc labeled antibody. Curr Radiopharm. 2014;7(2):84-90.

Gavande N, Kim HL, Doddareddy MR, Johnston GAR, Chebib M, Hanrahan JR. Design, synthesis, and pharmacological evaluation of fluorescent and biotinylated antagonists of ρ1 GABAC receptors. ACS Med Chem Lett. 2013;4(4):402-7.

Kaiser KP, Geuting B, Grossmann K, Vester E, Losse B, Antar MA, et al. Tracer kinetics of 15-(*ortho*-123/131I-phenyl)-pentadecanoic acid (oPPA) and 15-(*para*-123/131I-phenyl)-pentadecanoic acid (pPPA) in animals and man. J Nucl Med. 1990;31(10):1608-16.

Knapp FF, Ambrose KR, Goodman MM. New radioiodinated methyl-branched fatty acids for cardiac studies. Eur J Nucl Med. 1986;12(Suppl):S39-S44.

Lee BC, Kim DH, Lee JH, Sung HJ, Choe YS, Chi DY, et al. 99mTc(CO)3-15-[*N*-(acetyloxy)-2-picolylamino]pentadecanoic acid: A potential radiotracer for evaluation of fatty acid metabolism. Bioconj Chem. 2007;18(4):1332-7.

Machulla HJ, Stocklin G, Kupfernagel C, Freundlieb C, Hock A, Vyska K, et al. Comparative evaluation of fatty acids labeled with C-11, Cl-34 m, Br-77, and I-123 for metabolic studies of the myocardium: Concise communication. J Nucl Med. 1978;19(3):298-302.

Mathur A, Subramanian S, Mallia MB, Banerjee S, Samuel G, Sarma HD, et al. Synthesis and bio-evaluation of a new fatty acid derivative for myocardial imaging. Bioorg Med Chem. 2008;16(17):7927-31.

Mathur A, Sharma AK, Murhekar VV, Madhava B. Mallia MB, Pawade S, et al. Syntheses and biological evaluation of 99mTc-HYNIC-fatty acid complexes for myocardial imaging. RSC Adv. 2015;5(113):93374-85.

Messina SA, Aras O, Dilsizian V. Delayed recovery of fatty acid metabolism after transient myocardial ischemia: A potential imaging target for "Ischemic Memory". Curr Cardiol Rep. 2007;9(2):159-65.

Meszaros LK, Dose A, Biagini SCG, Blower PJ. Hydrazinonicotinic acid (HYNIC) - Coordination chemistry and applications in radiopharmaceutical chemistry. Inorg Chim Acta. 2010;363(6):1059-69.

Mirtschink P, Stehr SN, Walther M, Pietzsch J, Bergmann R, Pietzsch H-J, et al. Validation of 99mTc-labeled "4+1" fatty

Design and development of 6-hydrazinonicotinyl-fatty acid-mimetic ^{99m}Tc-complex as a potential myocardial imaging agent

acids for myocardial metabolism and flow imaging. Part 1: Myocardial extraction and biodistribution. Nucl Med Biol. 2009a;36(7):833-43.

Mirtschink P, Stehr SN, Walther M, Pietzsch J, Bergmann R, Pietzsch H-J, et al. Validation of ^{99m}Tc-labeled "4+1" fatty acids for myocardial metabolism and flow imaging. Part 2: Subcellular distribution. Nucl Med Biol. 2009b;36(7):845-52.

Montalescot G, Sechtem U, Achenbach S, Andreotti F, Arden C, Budaj A, et al. 2013 ESC guidelines on the management of stable coronary artery disease: the Task Force on the management of stable coronary artery disease of the European Society of Cardiology. Eur Heart J. 2013;34(38):2949-3003.

Morton DB, Griffiths PHM. Guidelines on the recognition of pain, distress and discomfort in experimental animals and an hypothesis for assessment. Vet Record. 1985;116(16):431-6.

Otto CA, Brown LE, Wieland DM, Beierwaltes WH. Radioiodinated fatty acids for myocardial imagine: Effects of chain length. J Nucl Med. 1981;22(7):613-8.

Schwenk RW, Luiken JJ, Bonen A, Glatz JF. Regulation of sarcolemmal glucose and fatty acid transporters in cardiac disease. Cardiovasc Res. 2008;79(2):249-58.

Tamaki N, Morita K, Kuge Y, Tsukamoto E. The role of fatty acids in cardiac imaging. J Nuc Med. 2000;41(9):1525-34.

Zeng H, Zhang H. Synthesis and biological evaluation of fatty acids conjugates bearing cyclopentadienyl-donors incorporated [^{99m}Tc/Re(CO)$_3$]$^+$ for myocardical imaging. Eur J Med Chem. 2014;72:10-7.